Roll-to-Roll Printing of Silver Oxide Pastes and Low Temperature Conversion to Silver Patterns

Sangki Chun,*,† Dmitry Grudinin,† Dongwook Lee,† Sang-Ho Kim,† Gi-Ra Yi,‡ and Inseok Hwang†

Information & Electronic Materials Institute, LG Chem Research Park, 104-1, Moonji-dong, Yuseong-gu, Daejeon, 305-380, Republic of Korea, Korea Basic Science Institute, Seoul, 136-713 Republic of Korea

Received September 19, 2008. Revised Manuscript Received November 20, 2008

This paper reports a continuous roll-to-roll printing of mesh patterns of silver oxide pastes on flexible polymer films and subsequent thermal treatment at 150 °C of the patterned pastes to convert to silver patterns. The pastes consist of silver(I) oxide particles, silver salt of tertiary fatty acid, $AgOCO-C(CH_3)_2-(CH_2)_n-CH_3$ and α-terpineol as the solvent. During the thermal process, nanosized silver particles were formed by the thermal reduction of silver oxide particles and the salt, followed by spontaneous condensation and further fusing, resulting in conductive silver films. The linear chain length n of silver salt, $AgOCO-C(CH_3)_2-(CH_2)_n-CH_3$, in the pastes, affects the electrical conductivity of resulting silver films significantly. An optimal range of linear chain length is found as $n = 5-9$. In the case of the paste with $n = 5$, an optimal weight fraction range of the salt in the paste is found as 20−40 wt % if the solvent composition is held constant at 20 wt %. Using the paste with an optimal composition, we obtained high-performance electromagnetic wave interference (EMI) shielding films that have shown a comparable shielding effectiveness as that made of conventional sputtered metallic silver films.

Introduction

Printable conducting materials or conductive inks attract a great deal of attention recently since they are prerequisite for flexible electronics including printed transistor circuits,[1−3] wearable electronics,[4] smart labeling system, known as radio frequency identification tags (RFID),[5] electromagnetic wave interference (EMI) shielding mesh films,[6] and many others. Unlike previously developed silver inks for high temperature annealing process, new applications in printable electronics require low temperature processable inks which can be formed into metallic films with high electrical conductivity ($>10^4$ S/cm) by thermally treating at a relatively low temperature at 150 °C or below. A conductive ink based on silver nanoparticles (<5 nm) has been proposed for this application since they can be melted at low temperature due to their high surface-to-volume ratio. Buffat et al.[7] and Li et al.[8] have demonstrated that highly conductive films ($\sim 10^4$ S/cm) were produced by annealing at 200 °C. However, a robust and simpler technique for industrial applications is yet to be developed for mass production of such small nanoparticles dispersed in a certain medium at low cost. An alternative approach based on the decomposition−reduction of metal−organic precursors was recently demonstrated, whereby metallic thin film could be produced by thermal treatment at low temperatures of 150 °C or below.[9,10] For instance, silver neodecanoate ink was printed by the ink-jet process and subsequent low-temperature thermal treatment, resulting in the specific electrical conductivity of silver between 2.1 and 3.3 × 10^5 S/cm.[9] However, in some industrial applications, it is required to prepare micrometer thick films. Since the ink-jet process could produce only a few hundred nanometer thick films, the printing process must be repeated several times for such thick films, which in turn is not cost-effective in addition to a stringent requirement for precise alignment of patterns in all succesive deposition steps. Moreover, wettability of substrates must be controlled and additional patterning processes are needed in the case of high-resolution patterns. To address these problems, a new type of paste, called *silver oxide paste*, was proposed more recently, which was essentially a mixture of micrometer-sized silver oxide particles and silver metallo-organic compounds.[10] While silver micropowder pastes, without silver metallo-organic compounds, have shown poor electrical

* Corresponding author. E-mail: sangki@lgchem.com.
† LG Chem Research Park.
‡ Korea Basic Science Institute.

(1) (a) Crawford, G. P., Ed. *Flexible Flat Panel Display*; John Wiley & Sons: West Sussex, U.K., 2005. (b) Klauk, H., Ed. *Organic Electronics: Materials, Manufacturing, and Applications*; Wiley-VCH: Weinheim, Germany, 2006.
(2) Li, Y.; Wu, Y.; Ong, B. S. *J. Am. Chem. Soc.* **2005**, *127*, 3266.
(3) Li, Y.; Wu, Y.; Ong, B. S. *J. Am. Chem. Soc.* **2007**, *129*, 1862.
(4) Weber, J.; Potze-Kamloss, K.; Hasse, F.; Detemple, P.; Voeklein, F.; Doll, T. *Sens. Actuators, A* **2006**, *132*, 325.
(5) Sangoi, T.; Smith, C. G.; Seymour, M. D.; Venkataraman, J. N.; Clark, D. M.; Kleper, M. L.; Kahn, B. E. *J. Dispers. Sci. Technol.* **2004**, *25*, 513.
(6) Vega, F. D. L.; Garbar, A.; Rottman, C.; Masoud, E.; Faulkner, B. *SID Symp. Dig. Tech. Pap.* **2006**, *37*, 1987.
(7) Buffat, P.; Borel, J.-P. *Phys. Rev. A* **1976**, *13*, 2287.
(8) Li, Y.; Wu, Y.; Ong, B. S. *J. Am. Chem. Soc.* **2006**, *128*, 4202.
(9) Deardon, A. L.; Smith, P. J.; Shin, D. Y.; Reis, N.; Derby, B.; O'Brien, P. *Macromol. Rapid Commun.* **2005**, *26*, 315.
(10) (a) Honda, T.; Okamoto, K.; Ito, M.; Endo, M.; Takahashi, K. U.S. Patent 6,942,825, 2005. (b) Honda, T. *Electron. Parts Mater.* **2003**, *42*, 97. (c) Lu, C.-A.; Lin, P.; lin, H.; Wang, S.-F. *Japn. J. Appl. Phys.* **2007**, *46*, 4179.

10.1021/cm802475m CCC: $40.75
Published on Web 12/30/2008

Scheme 1. Synthesis of Silver Neoalkanoate

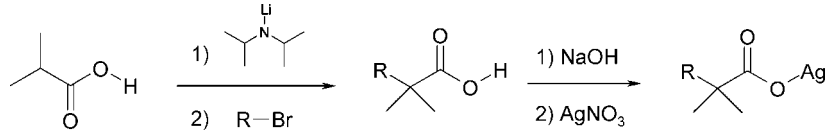

R = C_2H_5 ; C_4H_9; C_6H_{13}; C_8H_{17}; $C_{10}H_{21}$; $C_{12}H_{25}$

conductivities much lower than 10^4 S/cm, the mixture of silver oxide and metallo-ogranic compound has shown excellent processibility as well as high conductivity after thermal treatments.[10] However, it is still necessary to explore how silver oxide pastes are transformed into silver films, eventually leading us to find optimal compositions of the silver oxide pastes with better conductivity of final metallic films and lower treatment temperature. In particular, chemical structure and property of silver metallo-organic compounds in the pastes must be thoroughly investigated with respect to final silver films.

In this report, silver salts of tertiary fatty acid, AgOCO−$C(CH_3)_2$−$(CH_2)_n$−CH_3, called silver neoalkanoates for short, were used as the silver metallo-organic compounds. For systematically investigating their effects on the properties of final films, we have synthesized six silver neoalkanoates having different linear chain lengths wherein *n* is varied from 1 to 11. Upon using silver oxide pastes with these silver neoalkanoates, we have probed possible relationships between final silver film conductivity and the paste compositions having different linear chain lengths and relative amounts of the neoalkanoate. Finally, with optimal compositions of the paste so found, we demonstrate that a high-performance EMI shielding film could be produced by the roll-to-roll process on flexible polymer substrates.

Experimental Section

Instruments. NMR spectra were run on a Varian Utility Inova 500 spectrometer (500 MHz) using sample with concentration ~1% (^{1}H NMR) or ~5−10% (^{13}C NMR). IR spectra were obtained on a Bio-Rad FTS 3000 spectrophotometer. Mass spectra were recorded on a Finnigan LCQ MS spectrometer. Elemental analyses were performed using FLASH 112 Series CHNO Analyzer of Thermo Electron Corp. Thermalgravimetric analysis was conducted using Mettler-Toledo TGA 851e.

Synthesis of Starting Acid for Silver Neoalkanoates. As starting acids for silver neodecanoate, silver neododecanoate, silver neotetradecanoate and silver neohexadecanoate, 2,2-dimethyloctanoic acid, 2,2-dimethyldecanoic acid, 2,2-dimethyldodecanoic acid, and 2,2-dimethyltetradecanoic acid were prepared by modifying the synthetic routes reported in the literature that are for the preparation of 2,6-dimethylheptanoic acid[11] or 2,2,6,6-tetramethylheptadecanoic acid.[12] Our typical synthetic pathway is briefly outlined as follows (Scheme 1). Diisopropylamine was distilled from CaH_2 before use. To an ice-cooled solution of diisopropylamine (28 mL, 200 mmol) in dry THF (70 mL), a solution of *n*-butyl lithium in hexane (2.5 M, 80 mL, 200 mmol) was slowly added and was stirred at 0 °C for 30 min under nitrogen inside the glovebox. Isobutyric acid (9.3 mL, 100 mmol) was slowly added and stirred for 60 min, and the temperature rose gradually to room temperature in 30 min. The mixture was cooled down to 0 °C again and the corresponding isobutyl bromide (100 mmol) was slowly added, and the suspension was stirred at 0 °C for 1 h and then at room temperature for 12 h. The mixture was poured into ice-cold 10% hydrochloric acid in water (300 mL) and extracted with ethyl

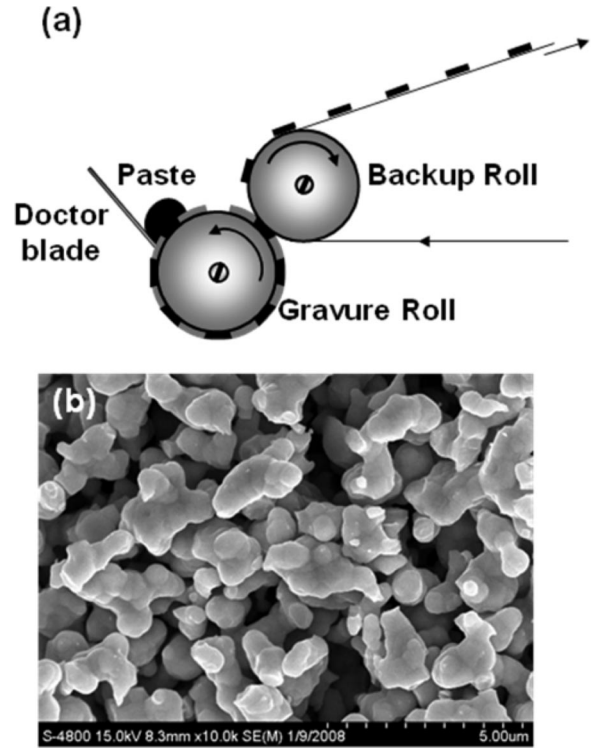

Figure 1. (a) Schematic diagram for roll-to-roll printing process. (b) Scanning electron micrograph of silver oxide microparticles.

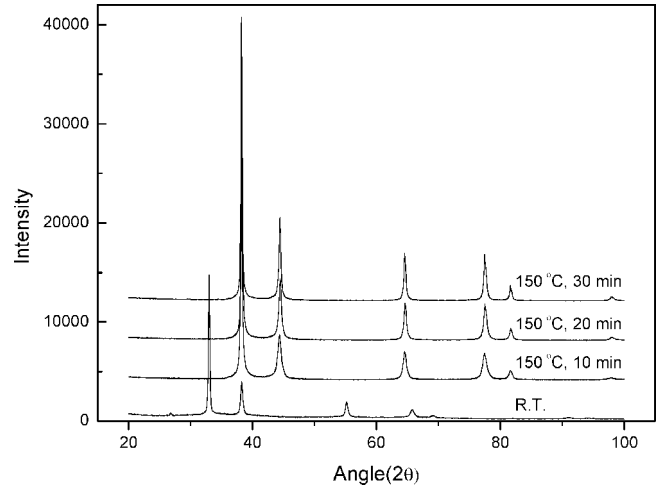

Figure 2. XRD spectra of silver films after heating process at 150 °C.

(11) ten Cate, A. T.; Dankers, P. Y. W.; Kooijiman, H.; Spek, A. L.; Sijbesma, R. P.; Meijer, E. W. *J. Am. Chem. Soc.* **2003**, *125*, 6860.
(12) ten Cate, A. T.; Kooijiman, H.; Spek, A. L.; Sijbesma, R. P.; Meijer, E. W. *J. Am. Chem. Soc.* **2004**, *126*, 3801.

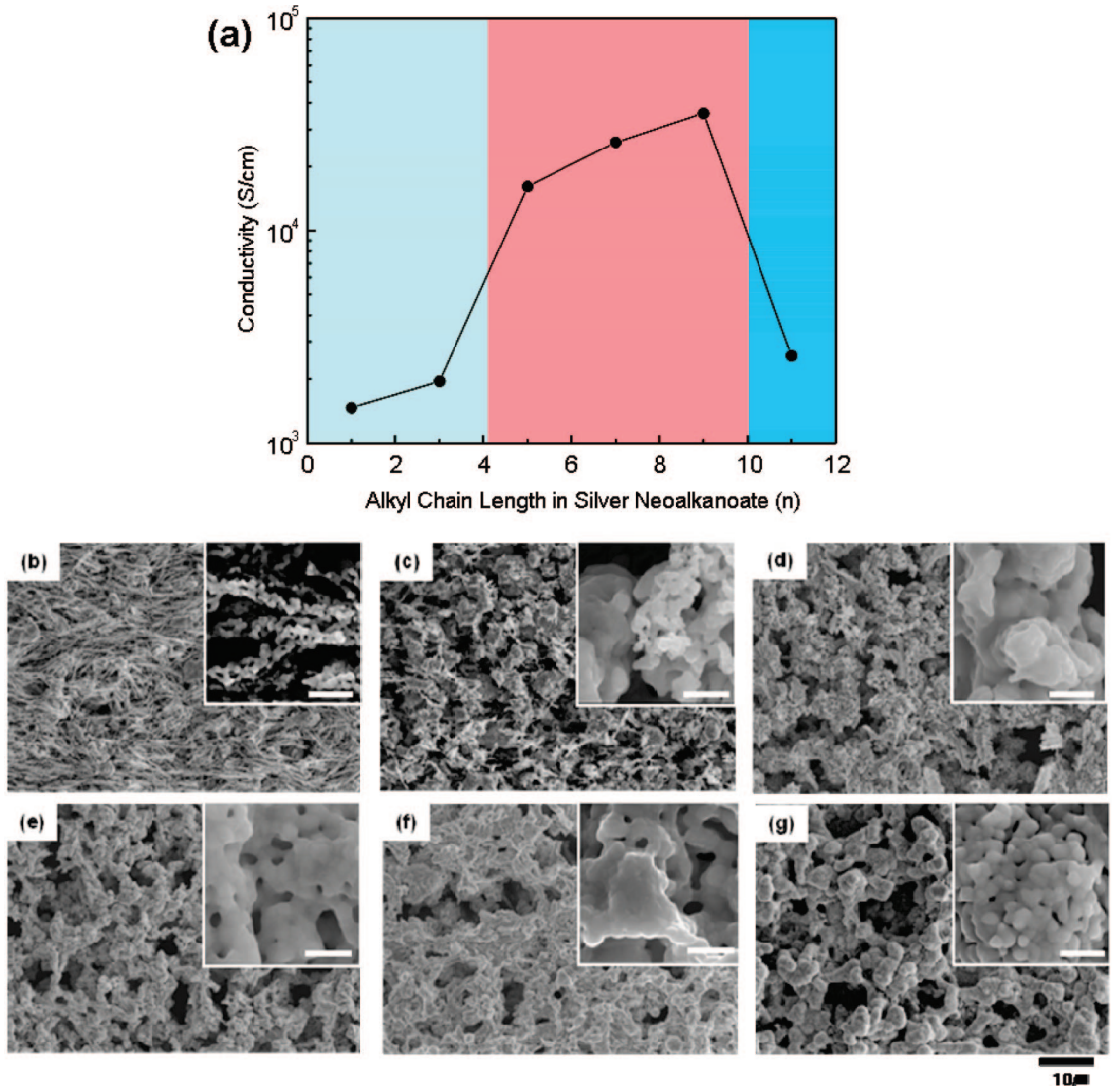

Figure 3. (a) Conductivity of silver film obtained after heating oxide pastes at 150 °C for 30 min, composed of silver oxide, silver salt, and α-terpineol (solvent), as a function of chain length n of linear part of silver neoalkanoate, $AgOCO-C(CH_3)_2-(CH_2)_n-CH_3$, on a semilog scale. Scanning electron micrographs of silver films obtained from oxide pastes with different linear chain length n of $AgOCO-C(CH_3)_2-(CH_2)_n-CH_3$: (b) $n = 1$, (c) $n = 3$, (d) $n = 5$, (e) $n = 7$, (f) $n = 9$, and (g) $n = 11$. Scale bars in insets are 500 nm.

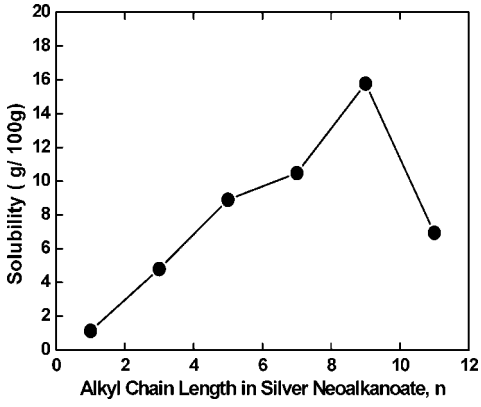

Figure 4. Solubility of silver salt in α-terpineol as a function of the linear chain length n.

acetate. The organic layer was washed with water, dried over Na_2SO_4, and distilled in vacuum.

Synthesis of Silver Neoalkanoates. Aqueous sodium hydroxide solution was slowly added to an equimolar amount of starting acid solution in methanol and kept stirring for 1 h. If needed for neutralization, dilute nitric acid was added to adjust the pH to 7. Then, an aqueous equimolar amount of silver nitrate was added and stirred for 1 h to afford a white precipitate of silver neoalkanoate. The precipitate was collected by filtration and washed with distilled water and methanol. Then, it was dried in a vacuum oven overnight. The precipitate was analyzed by NMR, IR, APCI-MS, and elemental analysis, and all results are summarized in Supporting Information.

Preparation of Silver Oxide Pastes. The silver oxide pastes used in this study were prepared by mixing Ag_2O particles (Kojundo, Japan) and silver neoalkanoates in α-terpineol (Kanto Chemical, Japan). All materials were mixed for 2 min and degassed for 1 min using a hybrid mixer (Thinky, AR-250, Japan). Subsequently, uniform pastes were prepared using a triple-roller grinder (Exakt 50, Germany), which breaks agglomerates of silver(I) oxide particles.

Preparation of Conductive Silver Film. The silver oxide paste was bar-coated on a PET film with a thickness of 30 μm and cured at a temperature of 150 °C for 30 min. A four point probe (Mitsubishi Chemical, MCP-T600, Japan) was used to measure the conductivity of silver film. The microscopic morphologies of silver films were observed under field emission scanning electron microscopy (Hitachi, s-4800, Japan).

Scheme 2. Illustration of Formation Hypothesis of Silver Films from the Printed Silver Oxide Pastes by a Simple Thermal Treatment at 150 °C

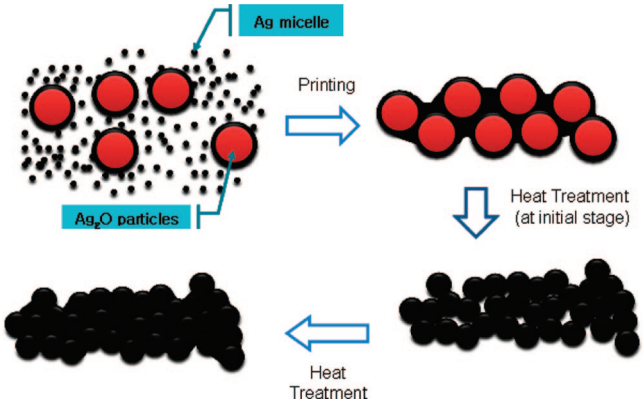

Results and Discussion

We now show how conductive patterned films can be produced by the roll-to-roll printing of the silver oxide pastes on flexible polyester substrates and subsequent simple thermal treatment at 150 °C for 30 min. The pastes were prepared by mixing silver oxide particles and silver neoalkanonate in α-terpineol. In Figure 1a is displayed a schematic diagram of the roll-to-roll printing process, and an SEM image of the silver oxide particles in the pastes is shown in Figure 1b. It should be noted that the particles are in an irregular and random structure, having average size of about 2 μm. Silver neoalkanoates with different linear chain lengths, $1 \leq n \leq 11$, were synthesized as described in the above. We show unambiguously that the silver oxide and neoalkanoate in the pastes reduce completely to metallic silver without leaving any residues by the simple heating at 150 °C under ambient conditions for 30 min. Evidence is put forth by Figure 2, XRD spectra of the heat treated film. To search for an optimal composition of the pastes resulting in the conductivity in a range of 10^4 S/cm, we have examined several factors affecting the final results. They are (1) the linear chain length n of neoalkanoate, (2) solubility of neoalkanoate in the solvent, α-terpineol, (3) time interval for the heat treatment, and (4) relative composition of the neoalkanoate and silver oxide in the pastes while keeping the solvent composition constant at 20 wt %. We now present the results for each factor examined. Parenthetically, all compositions are given by weight.

Linear Chain Length Dependence. The silver oxide pastes were prepared as follows. Silver oxide particles (50%) and Ag-neoalkanoate (16.7%) were mixed in α-terpineol with the aid of three-roll milling process. Once a homogeneous paste was obtained for each composition of n, it was bar-coated on a PET film. The wet thickness of paste film was about 30 μm on the average and final thickness of paste film was about 8 μm, and then metallic silver films were produced by heating them at 150 °C for 30 min. The specific electrical conductivities of the silver films were determined as described, and the results are displayed in Figure 3a. It is clear from the figure that linear alkyl chain length n of silver neoalkanoate has a significant effect on the final silver film conductivity. We can discern three distinguishable regimes. One with short chain lengths, $n = 1-3$, the next with optimum chain lengths, $n = 5$, 7, and 9, and the last with long chain length, $n = 11$. In the short n regime, the specific conductivity of the silver film is on the order of 10^3 S/cm. In the optimum regime of $n = 5$, 7, and 9, the conductivity reaches to the vicinity of 4×10^4 S/cm, not quite comparable to bulk Ag value of $\sim 6.3 \times 10^5$ S/cm.[10] In the last regime of $n = 11$, the conductivity reduces back down to that of the first regime. In short, there exists an optimum range of n at 5−9.

Parallel with the specific conductivity of the final silver films, we show SEM images of the neoalkanoate with six different chain lengths in Figure 3b−g. These images are consistent with the results in Figure 3a. In the short chain regime, silver particles are not fully connected. On the other hand, in the optimum regime, silver particles are well fused and connected. In the long chain limit, the particles are too granular with large voids that disrupt contiguous pathways for conduction. Examining further the microscopic morphologies of post-treatment silver particles for the three regimes of n, states of dispersion of the oxide particles mediated by the alkanoates in the paste may be responsible for the final states of silver. Thus, the solubility of alkanoate in α-terpineol is suspected to be a related factor of the linear chain length dependence.

Solubility of Neoalkanoates. Typically, an excess amount of silver neoalkanoate was dissolved in α-terpineol to obtain a saturated solution and then filtered through a 0.45 μm membrane filter, and then UV absorbance of filtered solution was measured at 210−220 nm. This was performed after 100-fold dilution by mixing a 100 μL aliquot of the filtered solution with 10 mL of α-terpineol. Absorbance data were referenced to that obtained with a solution made of 50 mg of silver neoalkanoates in 10 mL of α-terpineol. As shown in the plot of Figure 4, the solubility of silver neoalkanoate as a function of the chain length n is rather linear up to $n = 9$ and then falls off abruptly at $n = 11$. It is a signature for micelle formation of Ag-neohexadodecanoate ($n = 11$) in α-terpineol. It is noteworthy that α-terpineol does not degrade the surface of PET film at all.

We pause briefly for explanations of the results presented thus far. Combining chain length dependent silver particle morphologies with solubility of Ag-neoalkanoate in the solvent, it is now possible to propose a model as to how the final silver film conductivity depends on n and why the heating only at 150 °C suffices to reduce silver oxide to metallic silver. The starting point of our proposal is to assume that alkanoates in the paste act as a dispersant for the oxide particles. When $n = 1-3$, their solubility is insufficient to disperse them uniformly in the pastes such that their aggregates coexist with the partly covered oxide particles, resulting in isolated silver aggregate chains derived separately from the salt and oxide, as seen in Figure 3b,c. Next, when n is in the optimum range of 5−9, the neoalkanoates are assumed to be well dispersed and adsorbed on the oxide surfaces, thus rendering them as efficacious dispersants with the linear hydrocarbon chains acting as steric stabilizers. Once reduced, silver from both components are well integrated and interfused. The results are what we glean from

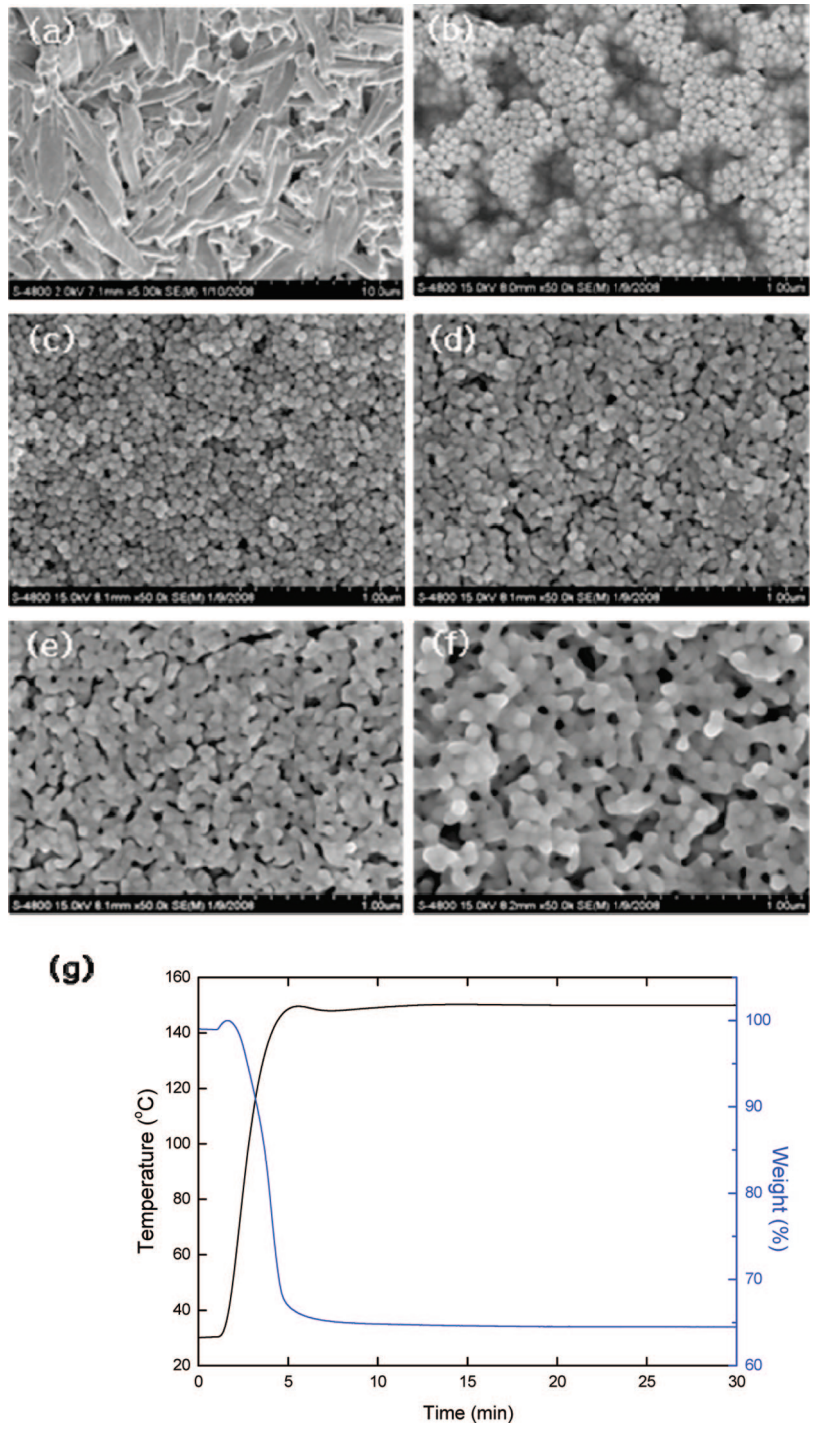

Figure 5. Scanning electron micrographs of the paste with a composition of 4:4:2 (oxide:salt:solvent) and resulting silver particles obtained by thermal treatment at 150 °C, for 0 min (a), 5 min (b), 10 min (c), 15 min (d), 20 min (e), and 30 min (f). (g) Thermogravimetric analysis of the same paste. Note that all mass losses are completed by $t = 5$ min.

Figure 3d−f. When n reaches 11, the neoalkanoate is postulated to self-assemble into micelles which compete with the adsorption onto the oxide surfaces, resulting in large void formation, as seen in Figure 3g. The proposal for micelle formation at $n = 11$ draws upon a precedence for silver stearate, reported by Dong et al.[13] Now, turning to the issue of a low temperature of 150 °C for the reduction of silver salt and oxide, giving rise to the deposition and fusing of silver particles, we note first that pure silver oxide cannot be reduced to metallic silver at a temperature lower than 200 °C.[14] On the other hand, it has been shown that once metallic shells or particles are formed around silver oxide partices, they in turn catalyze the reduction of the oxide at lower temperatures than 200 °C.[10c] Thus, we speculate that the sequence of the reduction−deposition process consists of reduction of silver ions of neoalkanoates on the oxide surface first that in turn form silver clusters or shells. These

(13) Dong, J.; Whitcomb, D. R.; McCormick, A. V.; Davis, H. *Nanotechnology* **2005**, *16*, S592.

(14) Kendall, J.; Fuchs, F. J. *J. Am. Chem. Soc.* **1921**, *43*, 2017.

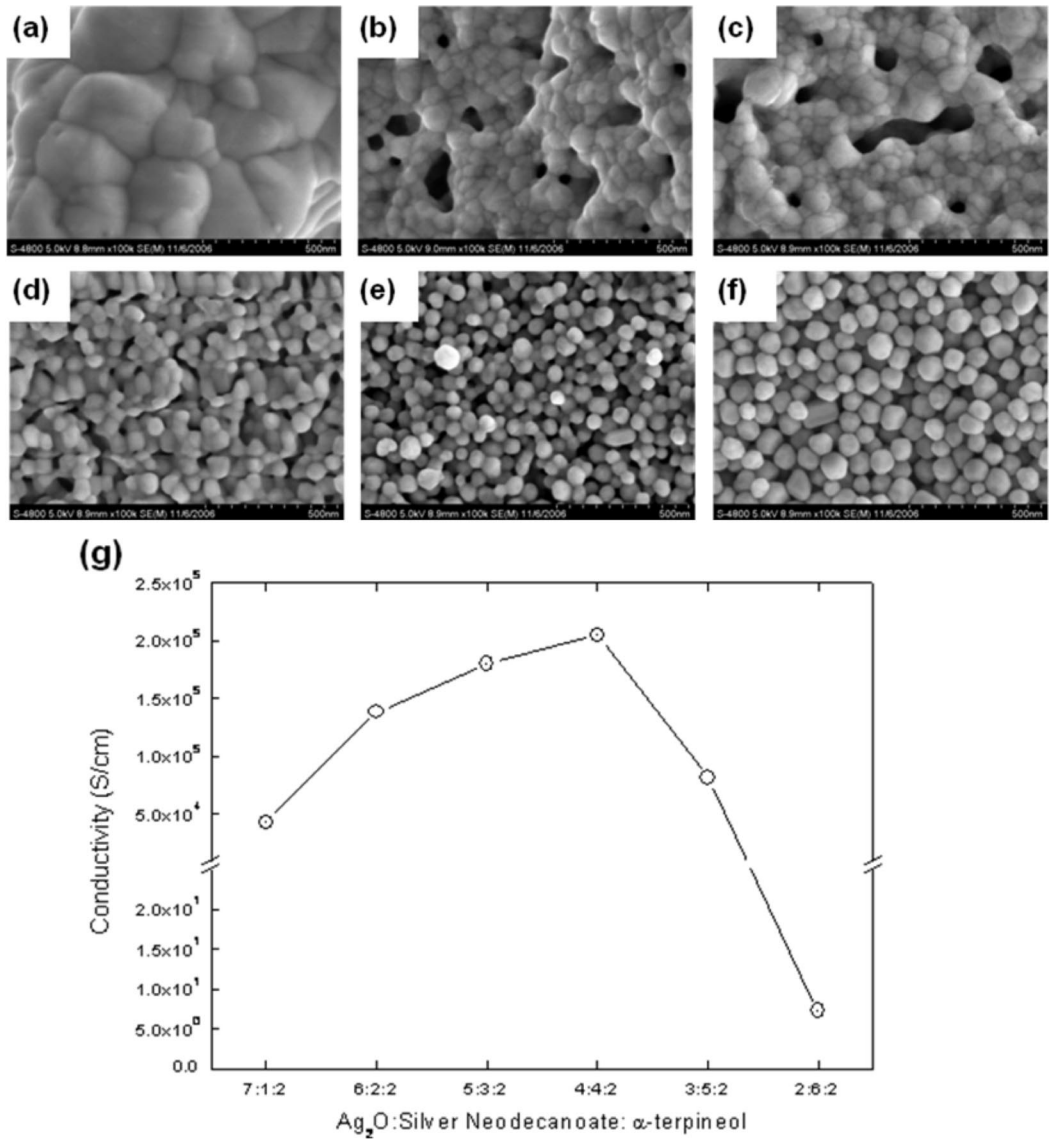

Figure 6. Scanning electron micrographs of silver film prepared using pastes with different proportions of silver oxide, silver neodecanoate ($n = 5$), and solvent: (a) 7:1:2, (b) 6:2:2, (c) 5:3:2, (d) 4:4:2, (e) 3:5:2, and (f) 2:6:2. (g) Conductivity of silver films formed from the pastes with the same compositions as a−f.

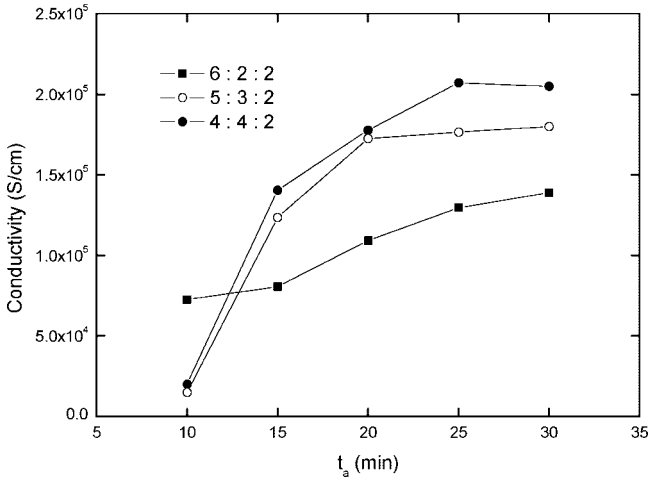

Figure 7. Conductivity of silver films obtained from the pastes with three optimum compositions, 6:2:2, 5:3:2, and 4:4:2 as a function of thermal treatment time t at 150 °C.

then catalyze the thermal reduction of the oxide particles, which is followed by fusion of silver particles, forming into networks. In Scheme 2, our speculation on the formation of silver film from silver oxide with proper silver neoalkanoate is illustrated.

Thermal Treatment Time Intervals. Sequence of transformation within a paste consisting of Ag-neodecanoate and Ag-oxide by thermal treatment at 150 °C is examined in detail. The paste was composed of Ag_2O particles, Ag-neodecanoate ($n = 5$), and solvent in a proportion of 4:4:2; the choice of this particular composition will be made clearer later. The time intervals were 5, 10, 15, 20, and 30 min, and resulting morphological changes are displayed by SEM in Figure 5a−f. It seems clear that the silver particle formation has run its course by the end of 5 min, and all subsequent steps are just particle growth and fusion into contiguous networks. Hence, we infer that all chemical changes should be completed within first 5 min. Lending support to this inference, we show results of thermogravimetric analysis in Figure 5g. It makes clear that all mass losses are complete within the same time interval of heating, hence no further oxide reduction and

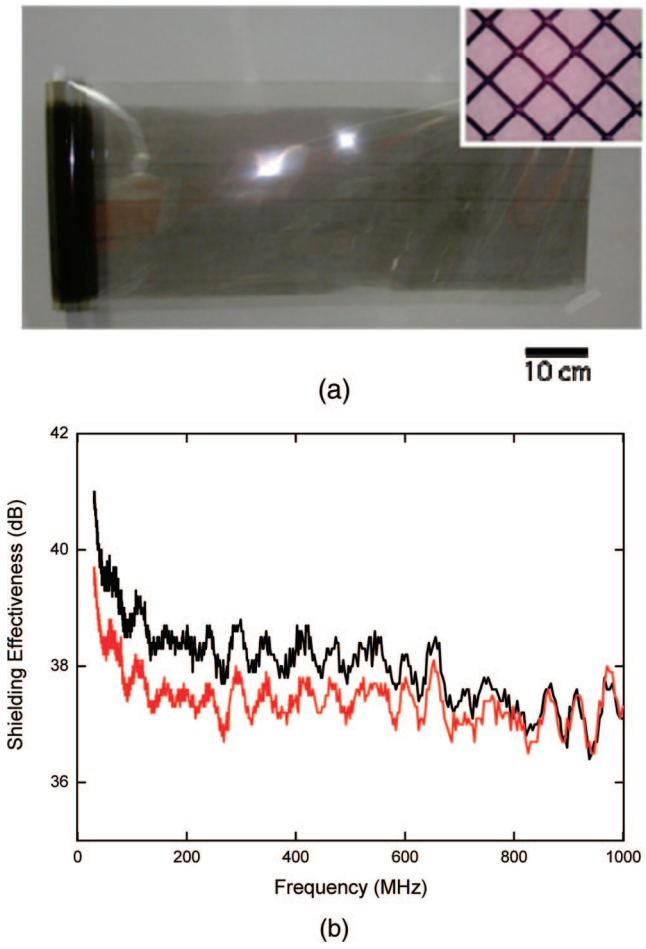

Figure 8. (a) Photograph of silver patterned films for EMI shielding applications by the roll-to-roll printing of the oxide pastes on PET film and subsequent thermal treatment at 150 °C for 30 min. Inset is optical micrograph of EMI mesh patterns. (b) EMI shielding effectivenesses of EMI film obtained using the roll-to-roll printing of a silver oxide paste with an optimum composition, 5:3:2 (black line) and EMI film prepared by sputtering method (red line).

vaporization of organic moieties should take place beyond this point of heating.

Relative Proportion of Oxide and Neoalkanoate. Next, we investigated the relative ratio of silver oxide and silver neodecanoates in the pastes. A series of paste compositions was made with ratios of oxide:salt of 7:1, 6:2, 5:3, 4:4, 3:5, and 2:6 while the solvent composition was held constant at 2, and all were bar-coated on PET film with 30 μm of wet thickness and identically heated at 150 °C for 30 min. Resulting silver films were probed by SEM, as shown in Figure 6a−f, where the oxide particles are decomposed and the silver salt transformed to small silver seed nanoparticles. In case of silver paste with 7:1 composition (a), we speculated that silver neoalkanoate was insufficient in amount to aid the reduction of silver oxide particles by dispersing on their surfaces to form nanosized seed silver particles. Thus, big silver particles were formed directly from the oxide particles, resulting in insufficient conducting networks. By constrast, when the silver salt was sufficient in amount relative to the oxide particles, as seen in Figure 6b−d, silver nanoparticles were formed in small enough in size so as to fuse well for conducting networks of silver. Lastly, when the salt was present in excess relative to the oxide particles, resulting in the product silver particles being large and well segregated, for their fusing temperature is likely higher than our processing temperture of 150 °C. These are exemplified in Figure 6e,f. In Figure 6g is displayed results of a parallel experiment for the electrical conductivity with the same set of compositions. Basically the optimum compositions at 6:2, 5:3, and 4:4 as seen in SEM are consistent with the observed conductivity plateau.

Having established the optimum composition range of 6:2, 5:3, and 4:4, we examine how they may differ in the heating process for reduction. Results for the conductivities for the three compositions of the pastes are plotted against the heating time t at 150 °C in Figure 7. The paste with a composition of 6:2 has a higher conductivity at the initial stage, whereas the final conductivity is less than the other two compositions. The pastes with larger proportions of silver salt have produced bigger silver particles. Therefore, the initial conductivity of the paste of a 4:4 composition is much less than others. However, after the silver particles were fused, it enhances abruptly at $t = 10-15$ min. Conductivity asymptotes with time at $t = 25-30$ min are also consistent with SEM of Figure 6b−d.

As stated at the outset of this section, the above four factors are presented as most relevant in producing the final silver films at the optimum. Finally, with use of the paste with one of the optimum compositions, i.e., 5:3 composition, we prepared EMI shielding film on PET films by the roll-to-roll printing process. For promoting adhesion between mesh pattern and PET film, isocyanate primer was coated on PET film before printing process. As shown in Figure 8a, mesh patterns of the paste on PET film were produced at a speed of 1 m/min and heated at 150 °C for 30 min through an in-line convection oven. As shown in the inset of Figure 8a, square mesh patterns with the thickness of 3 μm were successfully produced, in which pitch of line pattern was 300 μm and line width is 30 μm. We have determined shielding effectiveness of our mesh film using Network Analyzer (Agilent, N5230A, U.S.A.) following ASTM D4935-99. As shown in Figure 8b, our roll-printed silver mesh film compared favorably with conventional EMI shielding film prepared by sputtering method (sheet resistivity is 1.5 Ω/□) in terms of EMI shielding effectiveness over 100 to 1000 MHz.

Conclusions

We have used the mixture of silver oxide particles and silver salt of tertiary fatty acid (Ag-neoalkanoates) in α-terpineol as low-temperature processable pastes on flexible substrates. Their chemical compositions were systematically investigated by structurally varying silver neoalkanoate through the variations of chain length of linear portion of the tertiary fatty acid and compositions. Conductivities of resulting silver patterns are found to depend significantly on the linear chain length of silver neoalkanoates in the pastes. We have established the optimal range of linear chain length to be 5−9. Also, we found that the optimum compositions in the pastes, upon fixing the solvent at 20%, are 60%:20%, 50%:30%, and 40%:40% for the relative amounts of oxide:

salt. For higher compositions of silver salt, the size of the resulting silver particles was so large to render their melting temperature greater than the processing temperature. For lower compositions of the salt, it was not enough for lowering the reduction temperature of the oxide. Finally, using an optimal silver paste, we have successfully produced high-performance EMI shielding film over a large area continously by the roll-to-roll printing on flexible substrates and heating at 150 °C for 30 min.

Acknowledgment. We are grateful to Jungwon Park and Byungjoon Chae for assistance in recording SEM images. Gi-Ra Yi was supported by a grant from Korea Ministry of Knowledge Economy (10030038).

Supporting Information Available: NMR, IR, APCI-MA, and elemental analysis data for synthesized silver neoalkanoates (PDF). This material is available free of charge via the Internet of http://pubs.acs.org.

CM802475M